INTERNATIONAL JOURNAL FOR NUMERICAL METHODS IN FLUIDS, VOL. 8, 1183–1193 (1988)

LINEAR AND NON-LINEAR MECHANISMS IN BOUNDARY LAYER TURBULENCE

MARTEN T. LANDAHL

The Royal Institute of Technology, Stockholm, Sweden, and Massachusetts Institute of Technology, Cambridge, MA 02139, U.S.A.

SUMMARY

The different stages of bursting and evolution of the fluctuation field in a turbulent boundary layer are governed by mechanisms that may be identified as either predominantly linear, i.e. governed by linear interaction with the mean shear flow, or non-linear, i.e. with interaction between the fluctuation components also being important. Wave number–frequency spectra reveal the presence of damped wave modes that may be modelled from the Orr–Sommerfeld equation. Conditional sampled experimental data for streamwise velocity fluctuations in the wall layer obtained using the variable interval time averaging (VITA) method scale with the threshold level in a manner consistent with linearity. High-amplitude wall pressure peaks show an approximately linear relationship with the associated vertical velocity fluctuations. Non-linearity acts primarily in the near-wall region where the fluctuation velocity is relatively the highest.

INTRODUCTION

To predict directly from the Navier–Stokes equations even simple high-Reynolds-number turbulent flows, such as the boundary layer over a flat plate, is a task that continues to baffle the fluid mechanician. Because of the difficulties posed by the non-linearity of the problem and the complicated and poorly understood three-dimensional fluctuation field, in order to determine the mean properties of the turbulent flow, he is forced to resort to turbulence models in the form of semi-empirical relationships between the fluctuation field and the mean flow, or to seek some other approximate closure of the system of averaged equations. Direct numerical simulation has become possible in recent years with the advent of supercomputers, but the range of Reynolds numbers that can be covered with such simulations is quite limited and is likely to remain so in the foreseeable future. Therefore, although such simulations will enhance the understanding of the physics of turbulence, they are not ever likely to become a standard tool for the high-Reynolds-number situations encountered in engineering practice.

The non-linearity of the governing equations is responsible for the chaotic behaviour of the turbulence as well as for the large range of scales that appear. From both a fundamental and applied point of view it is therefore important to try to sort out in what mechanisms the non-linearity plays a large and essential role. Those in which non-linearity is weak may then possibly be handled in a simplified manner based on the small-perturbation equations.

0271–2091/88/101183–11$05.50

Received 27 July 1987
Revised 16 December 1987

In the past several attempts have been made to apply linear models to boundary layer turbulence. Sternberg[1] considered the fluctuation field in the near-wall region to be driven by the pressure fluctuations produced by the turbulence in the outer flow. By considering the fluctuation field as perturbations on the mean shear flow, approximated as a parallel one, Landahl[2] and Bark[3] formulated the fluctuation field in terms of a non-homogeneous Orr–Sommerfeld equation from which the wave properties of the turbulence could be studied.

In more recent work Landahl[4, 5] has demonstrated that a simple approximate linear inviscid model may reproduce quite well the sampled velocity signatures obtained in experiments with the use of the variable interval time averaged (VITA) technique. The recent experiments by Johansson *et al.*,[6] in which both the wall pressure and the streamwise and vertical velocity components were measured simultaneously, showed that the pressure peak scaled linearly with the vertical velocity component and also that the peak occurred at the time when the vertical velocity–mean shear interaction could be expected to be at a maximum, in consistency with a linear governing mechanism.

PARALLEL MEAN FLOW FORMULATION

The role of non-linearity in the dynamics of boundary layer turbulence may be at least partially understood from theoretical models similar to those used in the analysis of shear flow instability. Hence one treats the fluctuating field as a small but finite perturbation on a parallel mean flow, $U(y)\delta_{1i}$, by setting for the velocity $U_i(x_i,t)$ and pressure $P(x_i,t)$

$$U_i = U(y)\delta_{i1} + u_i(x_j,t), \qquad P = \bar{P} + p(x_i,t), \tag{1}$$

where $x_1 = x, x_2 = y, x_3 = z$ and $\bar{P}$ is the mean pressure. The assumption of a parallel mean flow is well justified since the turbulent eddies of interest have a length scale of the order of the boundary layer thickness over which the streamwise variation of the mean flow is small. Substitution into the Navier–Stokes equations then gives the following set of equations for the fluctuating components:

$$\bar{\mathrm{D}}u_i/\bar{\mathrm{D}}t + vU'\delta_{i1} = -\rho^{-1}\partial p/\partial x_i + \nu\nabla^2 u_i + \partial\tau_{ij}/\partial x_j, \tag{2}$$

$$\partial u_i/\partial x_i = 0, \tag{3}$$

where $v = u_2$, $U' = \mathrm{d}U/\mathrm{d}y$, $\bar{\mathrm{D}}/\bar{\mathrm{D}}t = \partial/\partial t + U\partial/\partial x$, $\nabla^2 = \partial^2/\partial x_j\partial x_j$, and where

$$\tau_{ij} = \langle u_i u_j \rangle - u_i u_j, \tag{4}$$

in which $\langle\ \rangle$ denotes ensemble average, may be regarded as fluctuating Reynolds stresses. Here the set (2) has been written in such a form that the non-linear terms, incorporated in τ_{ij}, may be thought of as driving the fluctuations. This may be brought out more clearly by eliminating p from the set (2) with the use of (3), which yields[2]

$$\bar{\mathrm{D}}\nabla^2 v/\bar{\mathrm{D}}t + U''\partial v/\partial x - \nu\nabla^4 v = q, \tag{5}$$

where $U'' = \mathrm{d}^2 v/\mathrm{d}y^2$ and

$$q = \nabla^2 T_2 - \partial^2 T_i/\partial x_i\partial x_2, \tag{6}$$

with

$$T_i = \partial\tau_{ij}/\partial x_j. \tag{7}$$

Since the non-linear terms involve higher spatial derivatives of the fluctuating velocities than the linear ones, one would expect that non-linear effects would be comparatively more important for the smaller scales than for the larger ones. Because the eddies involved tend to have much larger horizontal than vertical dimensions, i.e. to be 'flat' one may expect the terms involving the highest y-derivatives to give the major contribution to q. Hence from (6)

$$q \approx -(\partial^2/\partial y^2)[\partial(uv)/\partial x + \partial(vw)/\partial z]. \tag{8}$$

Measurements of the instantaneous uv during bursting carried out by Kim *et al.*[7] show that the Reynolds stresses are highly intermittent and large only in a thin layer near the wall. This is illustrated in Figure 1 taken from the paper by Bark.[3] (In the figure is also included his analytical fit to the data used in his calculation of the wave number–frequency spectra.) Corresponding results for the instantaneous stress component vw are not available, but one would expect that it will be similarly concentrated near the wall. A conceptual model that emerges is thus one in which the fluctuating flow field is governed by linear interaction, with the mean flow outside this layer but driven by the turbulence created in a thin active non-linear wall layer.

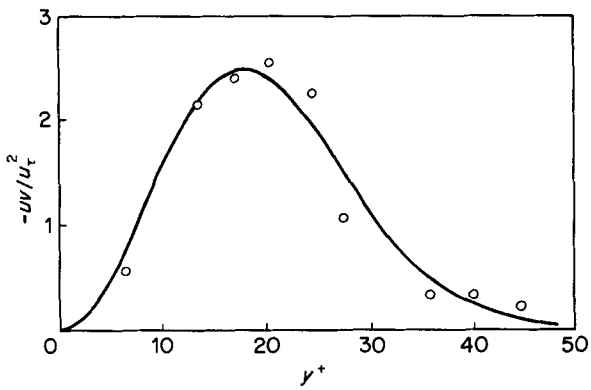

Figure 1. The uv component of the Reynolds stress tensor as a function of y^+ during bursting. ○ Measurements, Kim *et al.*[7] — Curve fit, Bark[3]

WAVE PROPERTIES

By application of a Fourier transform in x, z and t,

$$\hat{v} = (2\pi)^{-3/2} \int_{-\infty}^{\infty} \int \int v \exp[-\mathrm{i}(\alpha x + \beta z - \omega)] \mathrm{d}x \mathrm{d}z \mathrm{d}t, \tag{9}$$

one obtains the non-homogeneous Orr–Sommerfeld equation

$$L_{\mathrm{O-S}}(\hat{v}) = \hat{q}/\mathrm{i}\alpha, \tag{10}$$

where a caret denotes Fourier transform,

$$L_{\mathrm{O-S}}(\hat{v}) = (U - c)(\hat{v}'' - k^2 \hat{v}) - U'' \hat{v} - (1/\mathrm{i}\alpha R)(\mathrm{d}^2/\mathrm{d}y^2 - k^2)^2 \hat{v}, \tag{11}$$

$$k^2 = \alpha^2 + \beta^2, \qquad c = \omega/\alpha,$$

and where a prime denotes differentiation with respect to y.

For $q = 0$ the Orr–Sommerfeld equation for the mean flow is recovered. Numerical eigenvalue calculations[2, 3] show that the boundary layer mean velocity distribution is highly stable to small disturbances; hence the non-linear driving stresses as represented by $\hat{q}$ are essential for maintaining the turbulent fluctuations. A formal solution of (8), assuming that the non-linear source term $\hat{q}$ is known, may be constructed through expansion in terms of the eigenfunctions $\phi^{(n)}$ and eigenvalues $c^{(n)}$ of the homogeneous Orr–Sommerfeld problem as follows:[2]

$$\hat{v} = \sum_{n=1}^{\infty} A^{(n)} \phi^{(n)}(y), \tag{12}$$

where

$$A^{(n)} = \frac{1}{\mathrm{i}(\omega - \omega^{(n)}) I_n} \int_0^{\infty} q\, \phi^{(n)}\, \mathrm{d}y, \tag{13}$$

$\omega^{(n)} = \omega_{\mathrm{r}}^{(n)} + \mathrm{i}\omega_{\mathrm{i}}^{(n)} = \alpha c^{(n)}$, where $\phi^{(n)}$ are the eigensolutions of the Orr–Sommerfeld problem and $\phi^{(n)}$ their adjoints, and where

$$I_n = \int_0^{\infty} (\phi'^{(n)} \phi'^{(n)} + k^2 \phi^{(n)} \phi^{(n)}) \mathrm{d}y. \tag{14}$$

In this, contributions that may arise from the continuous spectrum have been ignored. The major contribution may be expected to come from the least damped eigenmode, denoted by superscript 0. The wave number–frequency spectrum Ψ_{vv} of v will be proportional to $|\hat{v}|^2$; hence

$$\Psi_{vv} \sim 1/|\omega - \omega^{(0)}|^2 = 1/[(\omega - \omega_{\mathrm{r}}^{(0)})^2 + (\omega_{\mathrm{i}}^{(0)})^2], \tag{15}$$

which is the spectral representation of a damped resonant wave system.

From v one may calculate the pressure and hence the other velocity components. As demonstrated below, for eddies of large horizontal dimensions compared with their thickness, the pressure is approximately linear in $\hat{v}$. Hence all the fluctuation components will vary with c in the same manner as $\hat{v}$ and thus have wave number–frequency spectra of the form (15).

By fitting a curve of the form (15) to the measured spectra, one can determine experimental values for both propagation velocity and damping for the waves. This was done by Bark[3] employing the experimental data from the pipe flow experiments of Morrison *et al.*[8] In Figure 2, reproduced from Bark's paper, the complex phase velocity $c = c_{\mathrm{R}} + \mathrm{i}c_{\mathrm{I}}$ thus obtained is compared with that calculated from the Orr–Sommerfeld equation for the mean velocity distribution. The agreement is good for the propagation velocity (c_{R}) but with the damping ($-\alpha c_{\mathrm{I}}$), being the more sensitive quantity to the experimental fits of the spectrum and of U'', somewhat underpredicted, although showing the correct trend with α.

VITA-EDUCED VELOCITY SIGNATURES

Conditional sampling techniques are often applied in experimental turbulence research in order to isolate characteristic and frequently appearing flow features ('coherent structures') for detailed study. The sampling condition, such as on threshold, velocity quadrant or short-time variance (variable interval time averaging, VITA), is used to establish the time of occurrence of an event, around which the sampling is then carried out. In this manner one may obtain an average time history of the event. What type of event one finds in this manner does of course depend on the sampling condition used.

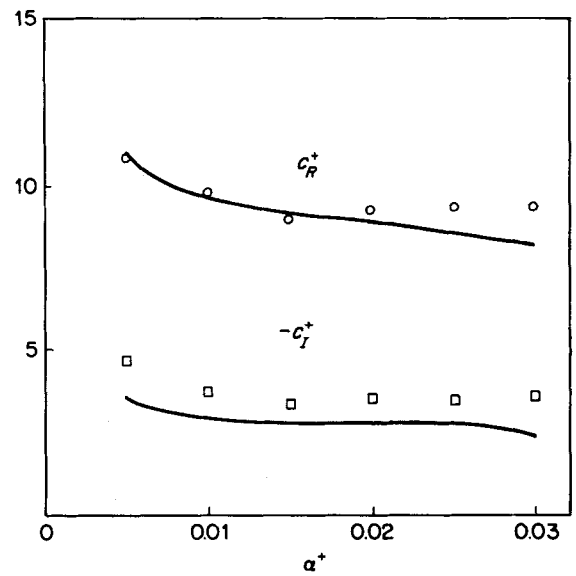

Figure 2. Real and imaginary parts of the downstream phase velocity. ○, □ Determined from experiments, Morrison *et al.*[8] — Orr–Sommerfeld computations, Bark[3]

In the VITA technique the sampling is carried out when the short-time variance of a fluctuating quantity, such as u, exceeds the root mean square by a selected threshold factor k, i.e.

$$\mathrm{var}(u, T, t_n) > k u_{\mathrm{rms}}^2, \tag{16}$$

where

$$\mathrm{var}(u, T, t) = (1/2T) \int_{t-T}^{t+T} u^2 \, \mathrm{d}t - \left((1/2T) \int_{t-T}^{t+T} u \, \mathrm{d}t \right)^2 \tag{17}$$

and t_n is the time of occurrence of the event around which the fluctuating component studied is sampled and presented as function of the time $\tau = t - t_n$ relative to the detection of the event. In most applications to date the velocity component selected for the sampling has been u. Its variance tends to become large when the flow experiences a strong local acceleration or retardation. This will occur when an inclined intense shear layer passes the measurement point. The VITA technique therefore tends to single out such structures.

The VITA-educed velocity signatures depends on both the threshold k and on the integration time T. As pointed out by Johansson and Alfredsson,[9] the time of integration serves as a filter which singles out structures of different duration, i.e. streamwise length scales. The sampled velocities for different k, when normalized by $\sqrt{(k u_{\mathrm{rms}}^2)}$, are found to collapse well onto one curve; this is particularly so if accelerating and decelerating events are treated separately.[9] As an example Figure 3 shows results obtained by Johansson and Alfredsson[9] in the wall region of a turbulent channel flow. In this figure the variables are expressed in viscous wall units.

The fact that the curves for different values of the threshold collapse so well onto a single curve is an indication that the process captured by the conditional sampling is a linear one. It follows from the sampling criterion (17) that the velocity amplitude range selected by a particular value of k is proportional to $\sqrt{(k u_{\mathrm{rms}}^2)}$. The good collapse for different k indicates that non-linear effects are

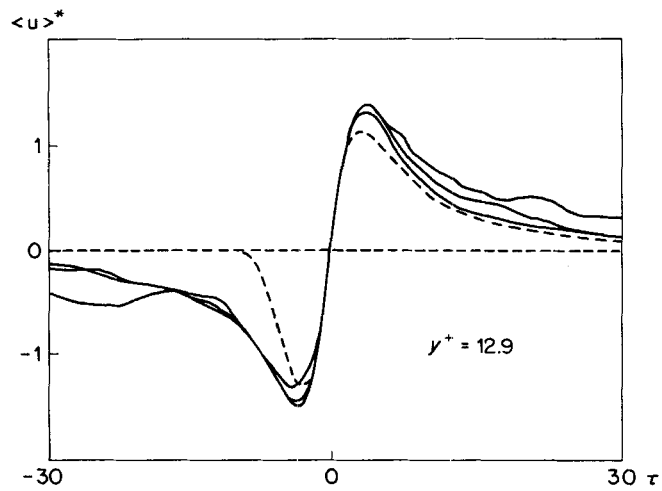

Figure 3. VITA-educed u-velocity signatures normalized by $\sqrt{(ku_{\text{rms}}^2)}$ for different threshold values.——Experiments, Johansson and Alfredsson[9] ----- Theory, Landahl[4]

comparatively small; if large, the signature of the sampled and normalized velocity would have depended strongly on the amplitude.

For the theoretical analysis one applies conditional sampling to the equations of motion, which results in

$$\tilde{\mathrm{D}}(\tilde{u}_i + U\delta_{i1})/\mathrm{D}t = -\rho^{-1}\partial\tilde{p}/\partial x_i + \nu\nabla^2\tilde{u}_i + \partial\tilde{\tau}'_{ij}/\partial x_j, \tag{18}$$

where a tilde denotes conditional average,

$$\tilde{\mathrm{D}}/\mathrm{D}t = \partial/\partial t + (U\delta_{1j} + \tilde{u}_j)\partial/\partial x_j \tag{19}$$

and

$$u_i = \tilde{u}_i + u'_i, \qquad \tilde{\tau}'_{ij} = \langle u_i u_j \rangle - \tilde{u}'_i\tilde{u}'_j, \tag{20}$$

a prime now denoting the non-coherent portion. By definition, the conditional average of the non-coherent fluctuation field u'_i is zero. The coherent velocity field $\tilde{u}_i$ satisfies continuity, as does u'_i.

In (18) the coherent field may be regarded as driven by the local and instantaneous Reynolds stresses produced by the non-coherent motion. The flow that results will of course depend on the condition used to educe the motion. However, certain general conclusions may be drawn from this formulation without the specific knowledge of the sampling criterion employed.

The time scale for an inviscid instability of a parallel flow is of the order $t_i = (\mathrm{d}U/\mathrm{d}y)^{-1}$, whereas the time scale of evolution of an eddy of streamwise length scale l_1 is the eddy convection time

$$t_e = l_1/U_e, \tag{21}$$

where U_e is the convection speed of the eddy. Typical values for eddies in the wall region are $l_1^+ > 100$, $U^+ \approx 10$, where '+' denotes viscous wall units. Hence, with $\mathrm{d}U^+/\mathrm{d}y^+ = O(1)$, $t_i/t_e \ll 1$. Since the time of creation of an eddy through a local instability is thus short compared with the time of evolution of the eddy, one could model the eddy development sequence approximately as a

shot noise process in which the local instability acts to set the initial v-velocity distribution which then evolves according to linear theory.

In Figure 3 are also included results for the VITA-educed u-component obtained from an approximate treatment of the linearized and inviscid version of (18).[4] In this, the effects of horizontal pressure gradients were neglected (see also below) and a simple model for the sampled Reynolds stresses due to the incoherent fluctuations was employed. Only the shape of the stresses need be assumed; the amplitude of the normalized and sampled velocity and the streamwise scale come out from the theory.

The agreement between theory and experiment is seen to be fairly good, except for the early times for which the theoretical model gives a much too rapid onset.

PRESSURE FLUCTUATIONS

By taking the divergence of the momentum equation (2), one obtains the well known Poisson equation for the pressure

$$\nabla^2 p/\rho = -2v_x U' - \partial^2(u_i u_j)/\partial x_i \partial x_j. \tag{22}$$

A formal solution of this is easily written down using the standard Green's function method. To assess the relative importance of the linear and non-linear terms, we apply a Fourier transform which gives

$$\hat{p}'' - k^2 \hat{p} = -2\mathrm{i}\alpha U' \hat{v} - \alpha^2 \hat{\tau}_{11} - \beta^2 \hat{\tau}_{33} - 2\alpha\beta\hat{\tau}_{13} - 2\mathrm{i}\alpha\hat{\tau}'_{12} - 2\mathrm{i}\beta\hat{\tau}'_{23}. \tag{23}$$

Multiplication of both sides by $\exp(-ky)$ and integration from $y = 0$ (the wall) to $y = \infty$ yields, after some integration by parts and application of the second momentum equation, the following expression for the pressure at the wall, $\hat{p}_w$:

$$\hat{p}_w = (2\mathrm{i}\alpha/k)\int_0^\infty U'\hat{v}\,\mathrm{e}^{-ky}\,\mathrm{d}y - \mu\hat{v}''_w/k$$
$$- \int_0^\infty [(\alpha^2\tau_{11} + \beta^2\hat{\tau}_{33} + 2\alpha\beta\hat{\tau}_{13})/k + 2\mathrm{i}\alpha\hat{\tau}_{12} + 2\mathrm{i}\beta\hat{\tau}_{23}]\mathrm{e}^{-ky}\,\mathrm{d}y. \tag{24}$$

All non-linear terms are collected on the second line. It is seen that they are all of one power higher in α, β or k than the linear terms. In a first-order long-wave approximation applicable to flat eddies, the non-linear terms may therefore be neglected.

That the relation between the fluctuating pressure and velocity field appears to be nearly linear is indeed the finding of Johansson *et al.*[6] in their recent measurements of the wall pressures in turbulent boundary layers and spots. As shown in Figure 4, they found that the sampled wall pressures, using the VITA condition (16) on u as a trigger, scaled with the threshold level as $\sqrt{k}$, i.e. in the same manner as u. The results for the pressures shown in Figure 4 were aligned with u through a two-step iteration procedure so as to remove the jitter in the p-signal. The phasing of the p-, and u- and v-signals was also found to be consistent with a linear model, with interaction between v and the mean shear constituting the pressure source.

A NON-LINEAR EJECTION MECHANISM

Strong non-linear effects may be expected to arise in the wall region due to local instabilities or due to large distortion of the flow away from its mean. Because of the short time scales to be expected for such processes, they are likely to be highly intermittent and localized in space. An interesting

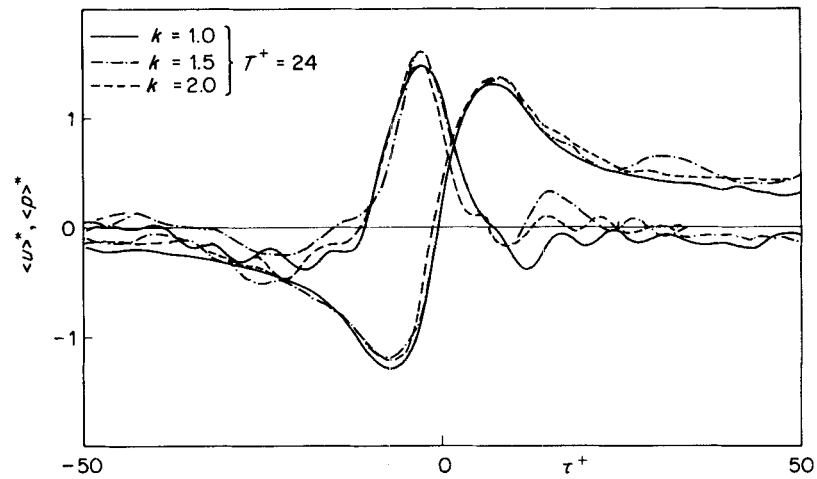

Figure 4. Aligned (two iterations) conditional averages of p_w and u at $y^+ = 15$ for VITA detection with various threshold levels. Note that the u- and p- averages here have been normalized with $K^{1/2}$ times the respective RMS. value (from Johansson *et al.*[6])

approach therefore is to view the set (2)–(4) from the point of view of intermittency. A turbulent burst in the near-wall region may be regarded as an isolated event which is only weakly influenced by a previous one. Then its evolution may be treated approximately as an initial value problem with the initial conditions set, possibly, by a previous localized instability. To study this non-linear initial value problem we write (2) as

$$\mathrm{D}(U\delta_{1i} + u_i)/\mathrm{D}t = -\rho^{-1}\partial p/\partial x_i + \nu\nabla^2 u_i + \partial\langle uv\rangle/\partial y, \tag{25}$$

where $\mathrm{D}/\mathrm{D}t = \partial/\partial t + (U\delta_{j1} + u_j)\partial/\partial x_j$ and with initial conditions

$$u, v, w = u_0, v_0, w_0 \quad \text{at } t = 0. \tag{26}$$

A formal solution of (25), (26) may be written down in terms of the Lagrangian co-ordinates ξ_i ($\xi_i = x_i$ for $t = 0$) as follows:[10]

$$U + u = U(\eta) + u_0(\xi_i) + \int_0^t (-\rho^{-1}\partial p/\partial x + \nu\nabla^2 u)\mathrm{D}t_1 + t\partial\langle uv\rangle/\partial y, \tag{27}$$

$$w = w_0(\xi_i) + \int_0^\tau (-\rho^{-1}\partial p/\partial z + \nu\nabla^2 w)\mathrm{D}t_1, \tag{28}$$

$$x = \xi + (U + u_0)t + \int_0^t (t - t_1)(-\rho^{-1}\partial p/\partial x + \nu\nabla^2 u)\mathrm{D}t_1 + (t^2/2)\partial\langle uv\rangle/\partial y), \tag{29}$$

$$z = \zeta + w_0 t + \int_0^t (t - t_1)(-\rho^{-1}\partial p/\partial z + \nu\nabla^2 w)\mathrm{D}t_1, \tag{30}$$

with the pressure obtained from

$$p = p_\infty + \rho\int_0^y (\mathrm{D}v/\mathrm{D}t)\mathrm{d}y_1 \tag{31}$$

and the vertical co-ordinate from

$$y = \int_0^{\eta} (1/A)\,\mathrm{d}\eta_1, \tag{32}$$

where

$$A = x_\xi z_\zeta - x_\zeta z_\xi \tag{33}$$

and the integration is to be carried out at constant x,z. Since the partial derivatives $x_\xi = \partial x/\partial \xi$, etc. can only be determined after the complete solution has been found, which in turn requires knowledge of the Eulerian co-ordinates x_i, the solution is only useful in situations where the pressure gradient and the viscous stresses are small so that their effect on the fluid element position is small, as would be the case for flat eddies.[10]

When the induced horizontal stresses are neglected, one finds the following simple approximate solutions:

$$U + u = U(\eta) + u_0(\xi,\eta,\zeta), \tag{34}$$

$$w = w_0(\xi,\eta,\zeta), \tag{35}$$

$$x = \xi + [U + u_0(\xi,\eta,\zeta)]t + \tfrac{1}{2}t^2\,\partial\langle uv\rangle/\partial y, \tag{36}$$

$$z = \zeta + w_0 t, \tag{37}$$

$$A = (1 + tu_{0\xi})(1 + tw_{0\zeta}) - t^2 u_{0\zeta} w_{0\xi}. \tag{38}$$

The effects of non-linearity in this model become particularly accentuated for conditions for which A is nearly zero in eqn (32), which may happen at a finite time after the onset. Such a case is illustrated in Figure 5, taken from Reference 11, which shows the evolution of an initial disturbance in the form of two pairs of counter-rotating vortices. The flow pattern revealed by the calculated consecutive fluid marker positions shows a remarkable similarity to that found by Kim *et al.*[7] for the ejection phase of the turbulent bursting sequence in their hydrogen bubble flow visualization experiments (reproduced in Figure 6). A closer examination of the theoretical model reveals that the high local vertical velocity results from local convergence of fluid elements in the horizontal planes forcing, through continuity, a large vertical velocity component (theoretically infinite in the simplified model). In the example shown the singularity occurs near $t = 4$ (the time is non-dimensionalized by the inverse of the wall shear rate), for which time the fluid elements have reached very large distances from the wall. The fact that such complicated non-linear behaviour can be simulated with such a simple model, assuming only conservation of mass and horizontal momentum, indicates that strong effects may arise from the cumulative non-linearities described by this model.

CONCLUSIONS

The presented analysis of experimental data on the basis of some simplified theoretical models indicates that the turbulent field may be described approximately as a linear system responding to the random forcing due to the non-linear bursting motion in a thin region near the wall involving predominantly small-scale motion.

In view of the short time scales to be expected during the intermittent phases of the bursting motion, viscous effects are likely to be unimportant for the non-linear driving mechanisms in the wall layer. Hence much understanding might be gained from the use of the inviscid equations. It

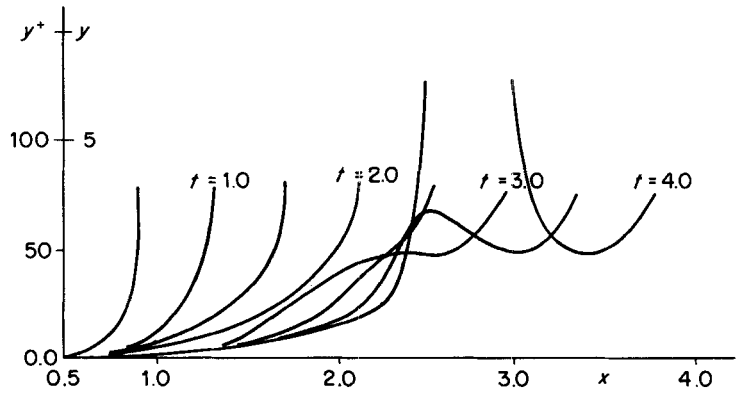

Figure 5. Bubble wire simulation of 40 marked particles originally at $x = 0{\cdot}5$, $z = 0$, shown at eight different times after the onset of an initial disturbance in the form of two counter-rotating streamwise vortices (after Landahl and Henningson[11])

Figure 6. Visualization of a bursting event with the aid of hydrogen bubbles from a pulsed wire (from Kim *et al.*[7])

has been speculated in the literature that the Euler equations may admit solutions that become singular at a finite time; the approximate treatment given above does indeed support such a possibility.

REFERENCES

1. J. Sternberg, 'A theory for the viscous sublayer of a turbulent fluid', *J. Fluid Mech.*, **13**, 241–271 (1962).
2. M. T. Landahl, 'A wave-guide theory for turbulent shear flow', *J. Fluid Mech.*, **29**, 441–460 (1967).
3. F. H. Bark, 'On the wave structure of the wall region of a turbulent boundary layer', *J. Fluid Mech.*, **70**, 229–250 (1975).
4. M. T. Landahl, 'On the dynamics of large eddies in the wall region of a turbulent boundary layer', in T. Tatsumi (ed.), *Turbulence and Chaotic Phenomena in Fluids*, Elsevier, 1984.
5. M. T. Landahl, 'Coherent structures in turbulence and Prandtl's mixing length theory', *Z. Flugwiss. Weltraumforsch.*, **8**, 233–242 (1984).
6. A. V. Johansson, J. Her and J. H. Haritonidis, 'On the generation of high-amplitude wall-pressure peaks in turbulent boundary layer and spots', *J. Fluid Mech.*, **175**, 119–142 (1987).
7. H. T. Kim, S. J. Kline and W. C. Reynolds, 'The production of turbulence near a smooth wall in a turbulent boundary layer', *J. Fluid Mech.*, **50**, 133–160 (1971).

8. W. R. B. Morrison, K. J. Bullock and R. E. Kronauer, 'Experimental evidence of waves in the sublayer', *J. Fluid Mech.*, **47,** 639–656 (1971).
9. A. V. Johansson and P. H. Alfredsson, 'On the structure of turbulent channel flow', *J. Fluid Mech.*, **122,** 295–314 (1982).
10. J. M. Russell and M. T. Landahl, 'The evolution of a flat eddy near a wall in an inviscid flow', *Phys. Fluids*, **27,** 557–570 (1984).
11. M. T. Landahl and D. S. Henningson, 'The effects of drag reduction measures on boundary layer turbulence structure—implications of an inviscid model', *AIAA Paper AIAA-85-0560*, 1985.